

# Transient ordering in the Gross-Pitaevskii lattice subject to an energy quench within the disordered phase

Andrei E. Tarkhov,<sup>1,2,\*</sup> A.V. Rozhkov,<sup>2,3</sup> and Boris V. Fine<sup>2,1,4,†</sup>

<sup>1</sup>Skolkovo Institute of Science and Technology, Bolshoy Boulevard 30, bld. 1, 121205 Moscow, Russia

<sup>2</sup>Moscow Institute of Physics and Technology, Institutskiy per. 9, Dolgoprudny, Moscow region 141700, Russia

<sup>3</sup>Institute for Theoretical and Applied Electrodynamics,  
Russian Academy of Sciences, Moscow 125412, Russia

<sup>4</sup>Institute for Theoretical Physics, University of Leipzig, Brüderstr. 16, 04103 Leipzig, Germany

(Dated: September 3, 2021)

Using the discrete Gross-Pitaevskii equation on a three-dimensional cubic lattice, we numerically investigate energy quench dynamics in the vicinity of the continuous  $U(1)$  ordering transition. The post-quench relaxation is accompanied by a transient order revival: during non-equilibrium stages, the order parameter temporarily exceeds its vanishing equilibrium pre-quench value. The revival is associated with slowly relaxing population of lattice sites aggregating large portions of the potential energy. To observe the revival, no preliminary fine-tuning of the model parameters is necessary. Our findings suggest that the order revival may be a robust feature of a broad class of models. This premise is consistent with the experimental observations of the revival in dissimilar classes of condensed matter systems.

*Introduction.* — Non-trivial transient ordering of an interacting many-body system in response to a sudden change of external conditions, a quench, has recently motivated extensive experimental and theoretical research [1–16]. Thermalization after a quench may take very long time [7, 16] and exhibit a rich variety of transient regimes [1–7, 15–21]. It can also be accompanied by the spontaneous formation of inhomogeneous structures [7, 10], the latter being regularly discussed in numerous papers dedicated, among other topics, to superconducting, charge-ordering, and magnetic transitions. There is also a mounting experimental evidence [1–7] that large variety of many-body systems may exhibit non-trivial transient ordering in response to a quench. The proposed interpretations of the non-equilibrium transient order revival/enhancement [7, 17, 21] are often based on the notion of multiple orders competing against each other both thermodynamically and kinetically.

Quite surprisingly, however, a very simple theoretical model with a single ordered phase is sufficient for observing the transient order revival. In this paper we illustrate this fact with the numerical simulation of the discrete Gross-Pitaevskii equation (DGPE) on a three-dimensional (3D) lattice, which exhibits an equilibrium phase transition below a certain temperature. In Fig. 1, we sketch the transient ordering of the system in the process of quenching. During the quench, the system is subjected to fast heating followed by fast cooling which ultimately brings the energy back to the pre-quench value. It is worth noting that before, during, and after the quench the energy remains within the high-temperature disordered phase on the phase diagram. Yet, we observe that the order parameter, absent in equilibrium due to high

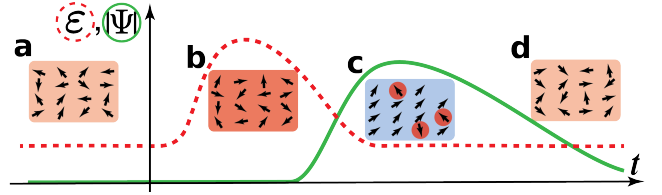


FIG. 1. Sketch of the quench procedure. The quench starts at  $t = 0$ . The system energy (dashed red line) initially grows, then it reverts to the pre-quench value. Due to high pre-quench energy density, the order parameter (green line) is zero before the quench, then grows rapidly due to the quench, relaxing back to zero after a long relaxation period. The cartoons depict internal system states at different stages of the quench. The color represents local energy density, with dark blue being the lowest, and bright red being the highest, the arrows correspond to the DGPE complex variables  $\psi_j$ . The equilibrium state, with moderately high energy density and vanishing order parameter, is shown in (a,d). Hot mid-quench state is in (b). Transient ordering is visualized in (c): the arrow directions are ordered, the energy density is inhomogeneous, with lumps of high energy shown by red color, the rest of the system being significantly cooler.

energy density at all stages of the quench, emerges during the quench, and persists long after that. We argue that the mechanism behind the observed transient ordering involves the nucleation of a small number of lattice sites with an atypically high concentration of energy. These sites are the 3D counterparts of the so-called discrete breathers that are shown to slow down thermalization in 1D DGPE chains [22–30]. Their concentration may be as little as several per cent, yet, they pull a significant fraction of total energy from the rest of the system, thereby temporarily cooling the latter below the temperature of the ordering phase transition, which in turn leads to the detected transient order. Below, we present

\* andrey.tarkhov@skoltech.ru

† fine.bv@mipt.ru

the detailed description of our simulations, substantiate our conclusions about the transient ordering mechanism and, finally, discuss the implications of our findings.

*The model.* — The DGPE system on a 3D cubic lattice is a classical dynamical system describing evolution of complex variables  $\psi_j(t)$  by the following equations

$$i \frac{d\psi_j}{dt} = - \sum_{k \in \text{NN}(j)} \psi_k + g |\psi_j|^2 \psi_j. \quad (1)$$

Here indices  $j$  and  $k$  label sites of the underlying 3D lattice, notation  $\text{NN}(j)$  denotes all sites that are nearest-neighbors to site  $j$ . The DGPE conserves total energy  $E = - \sum_j \sum_{k \in \text{NN}(j)} \psi_k^* \psi_j + \frac{g}{2} \sum_j |\psi_j|^4$ , where the kinetic energy is  $E^{(\text{kin})} = \sum_j E_j^{(\text{kin})} = - \sum_j \sum_{k \in \text{NN}(j)} \psi_k^* \psi_j$ , and the potential energy is  $E^{(\text{pot})} = \sum_j E_j^{(\text{pot})} = \frac{g}{2} \sum_j |\psi_j|^4$ . The norm (also called total number of particles)  $N = \sum_j n_j = \sum_j |\psi_j|^2$  is another integral of motion associated with the invariance of Eq. (1) relative to the global gauge transformation  $\psi_j \rightarrow e^{i\alpha} \psi_j$ . We eliminate redundancy in the DGPE parameters by fixing  $N = V$ , where  $V$  is the total number of sites, reducing the whole gamut of DGPE parameters to a single dimensionless constant  $g$ . The energy density,  $\varepsilon = E/V$ , is the only parameter that is being changed in the process of quenching.

*Equilibrium state of DGPE system.* — For sufficiently large lattice sizes and generic initial conditions the DGPE dynamics is chaotic, and exhibits ergodization that has been checked by various numerical ergodicity tests [31–35]. The averaged dynamics may be characterized in terms of entropy and temperature (see Appendix A) within microcanonical thermodynamic formalism. In equilibrium the microcanonical temperature  $T$  and  $\varepsilon$  are connected by monotonically growing invertible function  $\varepsilon = \varepsilon^{\text{eq}}(T)$ . This function, evaluated numerically and shown in Fig. 2 for  $g = 10$ , displays “a feature” at  $T_c \approx 1.92$ . It is associated with the transition into a low-temperature ordered state, characterized by the  $U(1)$  order parameter  $\Psi(t) = |\Psi(t)| e^{i\phi(t)} = \frac{1}{V} \sum_j \psi_j(t)$ . Equilibrium order parameter  $|\Psi| = |\Psi|^{\text{eq}}(T)$  is a decreasing function of  $T$  for  $T < T_c$ , vanishing above  $T_c$ .

*Transient revival.* — Before the quench, the system is prepared in an equilibrium state in a disordered phase at  $T > T_c$ . Then, the system is subjected to a fast energy increase followed by a cooling step, which brings the energy back to its pre-quench value. This is achieved by introducing a time-dependent gauge invariant term  $-K\psi_j D_j$  into the right-hand side of Eq. (1). Here  $D_j = i \sum_{k \in \text{NN}(j)} (\psi_k^* \psi_j - \psi_k \psi_j^*)$ , real function  $K = K(t, \kappa)$  is designed (see Appendix B) to guarantee that the total energy grows initially but later returns to the pre-quench value. Parameter  $\kappa$  controls the quench strength (see Appendix B). For our choice of the quench term, the quench affects directly the kinetic energy, but energy gets quickly redistributed to the potential energy due to the system’s natural dynamics.

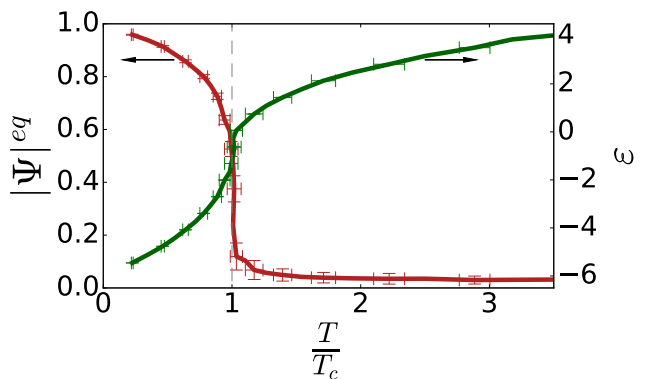


FIG. 2. Equilibrium energy density and the order parameter vs. the reduced temperature. For all plots,  $g = 10$ ,  $V = 10 \times 10 \times 10$ .

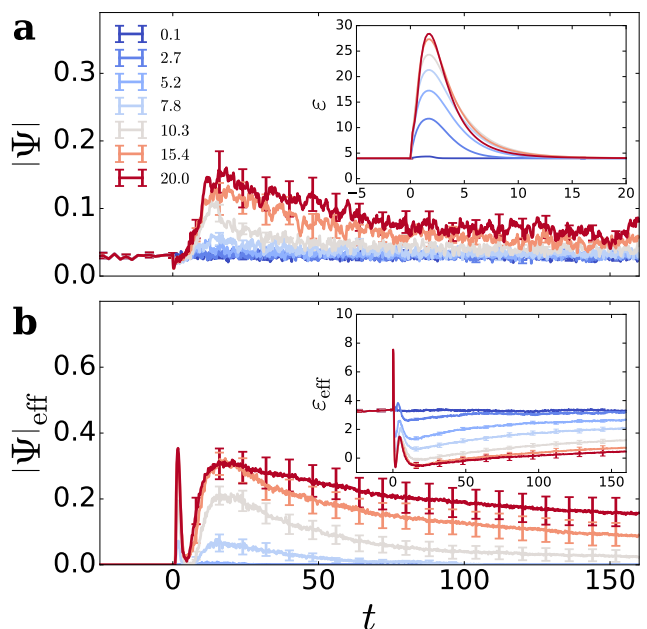


FIG. 3. Transient ordering. (a) The order parameter  $|\Psi|$ , barely discernible before the quench, is revived by quench (the energy quench plotted in the inset), and demonstrates long-lasting post-quench relaxation. (b) The equilibrium order parameter at the effective temperature of cold sites  $|\Psi|_{\text{eff}}(t)$  defined by Eq. (2) exhibits similar time evolution as  $|\Psi|(t)$  in panel (a). Inset: The effective energy density of cold sites  $\varepsilon^{\text{eff}}$ . The simulations are performed for  $g = 10$ ,  $V = 10 \times 10 \times 10$ , pre-quench temperature  $T/T_c \approx 3.7$ , the quench intensity  $\kappa$  plotted in the legend.

The system’s response to the quench is illustrated by Fig. 3(a). It shows  $|\Psi|(t)$  and  $\varepsilon(t)$  (in the inset) for  $g = 10$  and  $T/T_c \approx 3.7$ . When  $t < 0$ , the equilibrium value of  $|\Psi|$  is very small, determined by finite-size effects. Once the quench is launched at  $t = 0$ , the system energy spikes, the order parameter initially drops, but quickly starts growing. It reaches the maximum value ( $|\Psi| \approx 0.15$  for

the strongest quench) at  $t \sim 20$ . Remarkably, the post-quench relaxation of  $|\Psi|$  to its equilibrium value is very slow.

*The origin of the revival.* — As sketched in Fig. 1, the revival is associated with slowly relaxing lumps of potential energy nucleated during the quench. To substantiate this, we examine time evolution for the spatial distribution of the potential energy  $E_j^{(\text{pot})} = \frac{g}{2}|\psi_j|^4$ . In Fig. 4, the snapshots of this distribution in equilibrium and at two different time moments are presented ( $g = 10$ ,  $V = 10 \times 10 \times 10$ ,  $T/T_c \approx 3.7$ ,  $\kappa = 20$ ). While comparing equilibrium and non-equilibrium distributions, one notices the salient enhancement of the number of sites with very high values of the potential energy in far-from-equilibrium states. Energy does not spread evenly over the whole system, but instead preferably accumulates on a few sites. The relaxation displayed by these lumps of potential energy is sluggish: they tend to persist long after the quench is completed. During the post-quench dynamics the energy is conserved, hence, a finite population of the sites amassing significant fraction of energy implies that the rest of the system (all other sites) are effectively cooled down relative to the pre-quench temperature. For strong enough quenches, the cooler part of the system can temporarily find itself effectively at  $T < T_c$ , in the ordered phase. When the distribution of the potential energy approaches its equilibrium shape, the order revival is expected to disappear.

To make this discussion more quantitative, we introduce a cutoff energy density  $E_{th} \gg E/V$ , and use it to split all sites in a given state into two groups, “hot” and “cold”: any site  $j$ , for which  $E_j^{(\text{pot})} > E_{th}$ , is considered hot, otherwise, it is cold. If one sets  $E_{th} = 100$ , the equilibrium state at  $T/T_c \approx 3.7$ , contains  $x_{>}^{\text{eq}} \approx 0.55\%$  of hot sites, the energy accumulated there is  $E_{>}^{\text{eq}} \approx 685$ , which is approximately 17% of the total energy  $E = 4000$ . The quench acts to increase these values. For the state in Fig. 4(b), one has  $x_{>} \approx 1.3\%$  and  $E_{>} \approx 3500$ , which is approximately 88% of the total energy  $E = 4000$ . In such a case, the energy density of cold sites drops significantly below  $\varepsilon$ . Since the fraction of hot sites  $x_{>}$  is minuscule, the ensemble of the cold sites essentially coincides with the whole system. Thus, it is convenient to introduce the effective energy density  $\varepsilon_{\text{eff}}(t) = [E(t) - E_{>}(t)] / (1 - x_{>})V$ , plotted in the inset of Fig. 3(b), and effective temperature  $T_{\text{eff}} = T(\varepsilon_{\text{eff}})$  as approximate characteristics of such states. When  $T_{\text{eff}} < T_c$ , the emergence of the order parameter may be expected. Indeed, if we define “effective” order parameter as follows

$$|\Psi|_{\text{eff}} = |\Psi|^{\text{eq}}(T_{\text{eff}}), \quad (2)$$

we discover that the time evolution of  $|\Psi|_{\text{eff}}(t)$  is qualitatively the same as  $|\Psi|(t)$ , see Fig. 3(b).

*Discussion and conclusions.* — The DGPE on a sufficiently large lattice cluster represents a very simple model of a microcanonical thermodynamic system exhibiting an ordering transition into a  $U(1)$ -ordered phase.

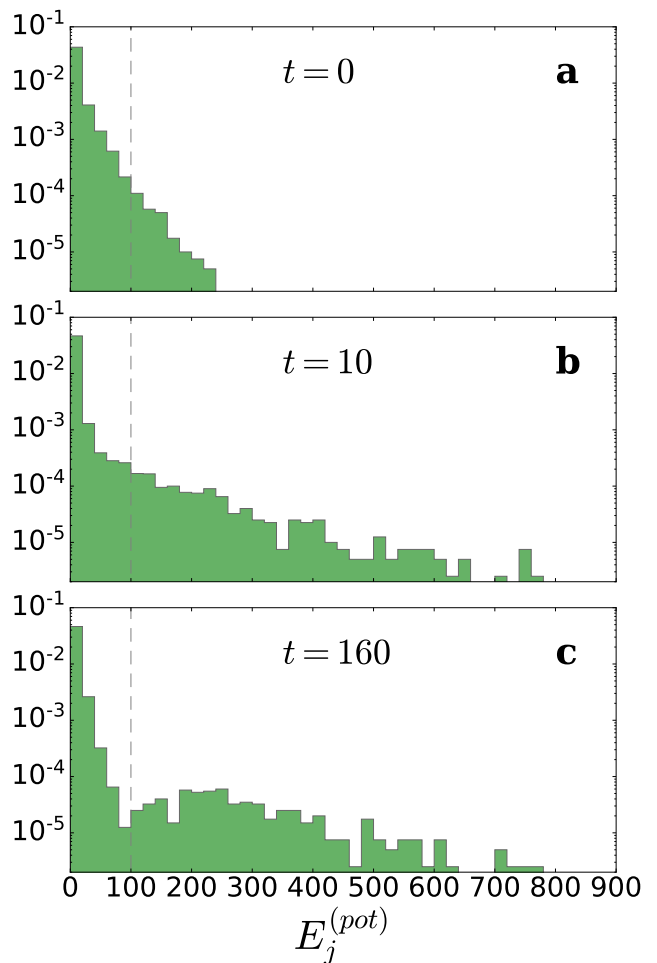


FIG. 4. Snapshots of the spatial distribution of local potential energy  $E_j^{(\text{pot})} = \frac{g}{2}|\psi_j|^4$ . (a) Equilibrium distribution. (b) Distribution immediately after the quench ( $t = 10$ ). (c) Distribution during the post-quench relaxation ( $t = 160$ ). The horizontal axis represents local potential energy, the vertical axis shows the concentration of sites with a given value of  $E_j^{(\text{pot})}$ . Presence of a larger number of sites with atypically large potential energy is visible in (b,c). The threshold energy  $E_{th} = 100$  is marked by vertical dashed lines. The simulation is performed for  $g = 10$ ,  $V = 10 \times 10 \times 10$ , pre-quench temperature  $T/T_c \approx 3.7$ , quench intensity  $\kappa = 20$ .

If a time-dependent perturbation, representing external drive, is included, one can use the DGPE to study non-equilibrium dynamics near the continuous transition. The model is characterized by the following three features: (i) in equilibrium, the model has a single ordered phase; (ii) by model’s very design, post-quench dynamics is inseparable from equilibrium state properties, as both are governed by the same set of differential equations; (iii) all equilibrium and post-quench properties are controlled entirely by the energy density  $\varepsilon = E/V$  and the interaction parameter  $g$ . Points (i-iii) imply that very little room for fine-tuning is available for the DGPE. Despite that, however, the model demonstrates transient

revival, a remarkable non-equilibrium phenomenon. The revival is a robust feature of the DGPE system.

We argued that the revival is associated with spontaneous nucleation of a small number of very “hot” sites during the quench. These sites act as “energy depot”, keeping the rest of the system colder than the nominal value of  $\varepsilon$  suggests. This allows for transient emergence of the order parameter in the “colder” part of the lattice. Note that, if we quench  $E^{(\text{pot})}$  instead of  $E^{(\text{kin})}$ , the revival should persist: due to the conservation of  $N$ , to increase the potential energy it is necessary to create highly inhomogeneous density distribution, rich in “hot” sites.

The simplicity of our model is to be contrasted with alternative approaches. One can try to explain the transient emergence of an unstable or metastable order using the following technique. A theoretical model with multi-order phase diagram is chosen and augmented with an *ad hoc* kinetics. Next, the kinetic coefficients of such a model are adjusted to direct the post-quench relaxation over a prearranged path on the phase diagram. The resultant kinetics demonstrates transient emergence of various ordered phases as the model state crosses phase boundaries on the phase diagram. The successful applications of this scheme can be found, for example, in Refs. 17 and 21. An obvious downside of this recipe is that it is greatly non-universal, demands a customized theory for every system exhibiting a revival, and, ultimately, requires justification for the fine-tuning of the coefficients. In our model, on the other hand, the revival requires neither specific design of the phase diagram, nor fine-tuning.

Current experimental research provides numerous examples of very dissimilar systems demonstrating transient emergence of an order. There are several cases of the revival of a  $U(1)$  order parameter. Specifically, Ref. 7 describes transient emergence of a charge-density wave order parameter. Revival of superconductivity in a cuprate material and in  $\text{K}_3\text{C}_{60}$  are reported in Refs. 1–4. The diversity of such systems suggests that a unifying mechanism behind the revival might be a fruitful theoretical avenue to explore. The DGPE with its simple and generic setup and natural  $U(1)$  ordered phase could be a first step in this direction.

Our numerical results clearly show that  $|\Psi|$  persists much longer than the duration of the quench, and its relaxation is remarkably sluggish, see Fig. 3(a). These theoretical findings are supported by recent experiments [5] on the superconducting order revival. The data demonstrate that the revived order relaxation may take long time.

To conclude, we numerically studied non-equilibrium evolution of the 3D DGPE model subjected to an energy quench. The order parameter revival was consistently observed, provided that the quench is strong enough. We offer a simple explanation for this phenomenon in terms of long-living breather-like lumps of potential energy. Such non-equilibrium behavior may be an intrinsic feature of broad class of dynamical models, and our find-

ings may shed light on experimental observations of the superconducting and charge-density wave revivals.

*Acknowledgments.* — This work was supported by a grant of the Russian Science Foundation (Project No. 17-12-01587).

## Appendix A: Microcanonical properties of DGPE

For vanishing disorder, “macroscopic features” of the DGPE can be described in terms of a microcanonical ensemble of all phase space states with fixed  $E$  and  $N$ . The microcanonical temperature is defined as:

$$\beta \equiv \frac{1}{T} \equiv \frac{\partial S}{\partial E}, \quad (\text{A1})$$

where  $S$  is the microcanonical entropy proportional to the logarithm of the volume of the energy shell  $w(E)$ ,

$$S \equiv \log \left[ \frac{w(E)}{(2\pi\hbar)^{V-\frac{1}{2}}} \right], \quad (\text{A2})$$

the Boltzmann’s constant is set to be equal to unity,  $k_B \equiv 1$ . The original definition of microcanonical temperature from conservative dynamics for an ergodic system reads [36–39]:

$$\frac{1}{T(E)} \equiv \lim_{t \rightarrow \infty} \frac{1}{t} \int_0^t d\tau \Phi(\mathbf{R}(\tau)), \quad (\text{A3})$$

where  $\mathbf{R}(\tau)$  is a phase space trajectory and the observable

$$\Phi \equiv \nabla \left( \frac{\nabla \mathcal{H}}{\|\nabla \mathcal{H}\|^2} \right), \quad (\text{A4})$$

is representative of the geometric curvature of the Hamiltonian on the energy shell. For practical calculation of microcanonical temperature, we adapt a numerical recipe, developed for classical spin lattices with one integral of motion [40] and consistent with the analytical approach [36, 37], to the calculation of the microcanonical temperature of the DGPE lattices with two integrals of motion. The original idea is to replace the functional in Eq. (A4) with its approximate numerical value by sampling the vicinity of the point in phase space  $\mathbf{R}(\tau)$ , and generating an ensemble of energy realizations, corresponding to each sample point. Then, by calculating the variance of energy fluctuations  $\langle \Delta E^2 \rangle$  and the mean fluctuation  $\langle \Delta E \rangle$ , one can extract the local approximation to  $\Phi(\mathbf{R})$  as

$$\Phi(\mathbf{R}) \equiv \frac{2\langle \Delta E \rangle}{\langle \Delta E^2 \rangle}. \quad (\text{A5})$$

We note that  $\langle \Delta E \rangle \neq 0$  due to the fact that, in general, there are exponentially more states above the energy shell than below it, which in turn reflects the fact that the

entropy in Eq. (A1) is proportional to the logarithm of the energy shell volume, and the temperature is positive. The temperature is then calculated as the time average along the phase space trajectory of Eq. (A5),  $1/T = \bar{\Phi}$ .

We use Eq. (A5) with an additional constraint due to the fixed second integral of motion, the number of particles, hence, when sampling the vicinity of a phase space point, we sample only the vicinity on the shell of a fixed number of particles,  $\langle \dots \rangle_N$ , which gives

$$T = \frac{\langle \Delta E^2 \rangle_N}{2\langle \Delta E \rangle_N}. \quad (\text{A6})$$

This equation acts as a practical definition of micro-canonical temperature. It satisfies all properties expected of temperature, and can be implemented numerically for a DGPE system with and without disorder. We will use Eq. (A6) to characterize DGPE equilibrium.

## Appendix B: Energy quench

The quench is performed on a DGPE system prepared in equilibrium. During the quench, the system's energy experiences quick rise and fall within a limited time interval. To allow for time variation of  $E$ , the DGPE must be modified to include time-dependent term:

$$i \frac{d\psi_j}{dt} = - \sum_{k \in \text{NN}(j)} \psi_k + g |\psi_j|^2 \psi_j - K \psi_j D_j, \quad (\text{B1})$$

$$\text{where } D_j = D_j^* = i \sum_{k \in \text{NN}(j)} (\psi_k^* \psi_j - \psi_k \psi_j^*), \quad (\text{B2})$$

and  $K = K(t, \kappa)$  is a real-valued function. The last term in Eq. (B1) is introduced to control the variation of  $E$  during the quench. Note that Eq. (B1), being gauge invariant, conserves  $N$ . The structure of the pump term is complicated and does not lend itself to immediate intuitive interpretation. To appreciate it, we can calculate  $\dot{E}^{(\text{kin})}$  and  $\dot{E}^{(\text{pot})}$  for dynamical equations (B1), and convince ourselves that  $\dot{E}^{(\text{kin})}$  acquires additional contribu-

tion  $-K \sum_j D_j^2$ , while the expression for  $\dot{E}^{(\text{pot})}$  is unaffected by the pump term. Thus, a quench described by Eq. (B1) impacts primarily the kinetic energy. Of course, since the system allows exchange between the two types of energy, altering  $E^{(\text{kin})}$  ultimately changes  $E^{(\text{pot})}$  as well. In the main text, we argue that our conclusions about the transient revival holds true if we pump  $E^{(\text{pot})}$  instead of  $E^{(\text{kin})}$ .

Since  $\dot{E} = \dot{E}^{(\text{kin})} + \dot{E}^{(\text{pot})} = -K \sum_j D_j^2$ , we conclude that the sign of  $K(t, \kappa)$  controls the increase/decrease of the total energy. Thus,  $K$  must be negative when the system heats, and positive during the cooling stage. We additionally demand that the energies of the system before and after the quench are identical. Function  $K(t, \kappa)$  compatible with these requirements is

$$K(t, \kappa) = -\theta(t) \left[ \kappa \frac{\gamma_2 e^{-\gamma_2 t} - \gamma_1 e^{-\gamma_1 t}}{\gamma_2 - \gamma_1} - \theta(t - t^*) \gamma \left( 1 - e^{-\gamma_2(t-t^*)} \right) \frac{E(t) - E_0}{E^* - E_0} \right], \quad (\text{B3})$$

where  $\theta(t)$  is the Heaviside step-function,  $\kappa$  is the parameter controlling the quench strength (in our simulations,  $\kappa$  spans the range from 0.1 to 20). Numerical values of  $\gamma$ 's are  $\gamma = 0.01$ ,  $\gamma_1 = 1$ , and  $\gamma_2 = 0.3$ . The second term in Eq. (B3) is added to guarantee that the energy after the quench is the same as before the quench. Here,

$$t^* = \frac{1}{\gamma_1 - \gamma_2} \log \left( \frac{\gamma_1}{\gamma_2} \right) \quad (\text{B4})$$

is the time moment at which  $K(t, \kappa)$  crosses zero and changes sign,  $E_0$  is the pre-quench energy of the system, while  $E(t)$  is the energy at time  $t$ , and  $E^* = E(t^*)$ . For further details one can refer to the source code published in a GitHub repository [41].

Before the quench, the system is prepared in an equilibrium low-energy state. In the first step of the quench the system is subjected to fast energy increase. The duration of such a pump stage is controlled by  $\gamma_2$ . In the cooling step (its duration is regulated by  $\gamma_1$ ) the energy is brought back to its pre-quench low value. Energy density evolution  $\varepsilon = E(t)/V = \varepsilon(t)$  is plotted in the main text.

- 
- [1] D. Fausti, R. I. Tobey, N. Dean, S. Kaiser, A. Dienst, M. C. Hoffmann, S. Pyon, T. Takayama, H. Takagi, and A. Cavalleri, Light-induced superconductivity in a stripe-ordered cuprate, *Science* **331**, 189 (2011).
- [2] C. R. Hunt, D. Nicoletti, S. Kaiser, T. Takayama, H. Takagi, and A. Cavalleri, Two distinct kinetic regimes for the relaxation of light-induced superconductivity in  $\text{La}_{1.675}\text{Eu}_{0.2}\text{Sr}_{0.125}\text{CuO}_4$ , *Phys. Rev. B* **91**, 020505 (2015).
- [3] M. Mitrano, A. Cantaluppi, D. Nicoletti, S. Kaiser, A. Perucchi, S. Lupi, P. Di Pietro, D. Pontiroli, M. Riccò, S. R. Clark, D. Jaksch, and A. Cavalleri, Possible light-induced superconductivity in  $\text{K}_3\text{C}_{60}$  at high temperature, *Nature* **530**, 461 (2016).
- [4] A. Cantaluppi, M. Buzzi, G. Jotzu, D. Nicoletti, M. Mitrano, D. Pontiroli, M. Riccò, A. Perucchi, P. Di Pietro, and A. Cavalleri, Pressure tuning of light-induced superconductivity in  $\text{K}_3\text{C}_{60}$ , *Nat. Phys.* **14**, 837 (2018).
- [5] M. Budden, T. Gebert, M. Buzzi, G. Jotzu, E. Wang, T. Matsuyama, G. Meier, Y. Laplace, D. Pontiroli, M. Riccò, F. Schlawin, D. Jaksch, and A. Cavalleri, Evidence for metastable photo-induced superconductivity in  $\text{K}_3\text{C}_{60}$ , *Nat. Phys.* **17**, 611 (2021).
- [6] J. Zhou and L. Hsiung, Long-term phase instability in a water-quenched uranium alloy, *J. Mater. Res.* **21**, 904

- (2006).
- [7] A. Kogar, A. Zong, P. E. Dolgirev, X. Shen, J. Straquadine, Y.-Q. Bie, X. Wang, T. Rohwer, I.-C. Tung, Y. Yang, R. Li, J. Yang, S. Weathersby, S. Park, M. E. Kozina, E. J. Sie, H. Wen, P. Jarillo-Herrero, I. R. Fisher, X. Wang, and N. Gedik, Light-induced charge density wave in  $\text{LaTe}_3$ , *Nat. Phys.* **16**, 159 (2020).
  - [8] A. Zong, X. Shen, A. Kogar, L. Ye, C. Marks, D. Chowdhury, T. Rohwer, B. Freelon, S. Weathersby, R. Li, J. Yang, J. Checkelsky, X. Wang, and N. Gedik, Ultrafast manipulation of mirror domain walls in a charge density wave, *Sci. Adv.* **4**, 10.1126/sciadv.aau5501 (2018).
  - [9] A. Zong, P. E. Dolgirev, A. Kogar, E. Ergeçen, M. B. Yilmaz, Y.-Q. Bie, T. Rohwer, I.-C. Tung, J. Straquadine, X. Wang, Y. Yang, X. Shen, R. Li, J. Yang, S. Park, M. C. Hoffmann, B. K. Ofori-Okai, M. E. Kozina, H. Wen, X. Wang, I. R. Fisher, P. Jarillo-Herrero, and N. Gedik, Dynamical slowing-down in an ultrafast photoinduced phase transition, *Phys. Rev. Lett.* **123**, 097601 (2019).
  - [10] A. Zong, A. Kogar, Y.-Q. Bie, T. Rohwer, C. Lee, E. Baldini, E. Ergeçen, M. B. Yilmaz, B. Freelon, E. J. Sie, H. Zhou, J. Straquadine, P. Walmsley, P. E. Dolgirev, A. V. Rozhkov, I. R. Fisher, P. Jarillo-Herrero, B. V. Fine, and N. Gedik, Evidence for topological defects in a photoinduced phase transition, *Nat. Phys.* **15**, 27 (2019).
  - [11] R. Yusupov, T. Mertelj, V. V. Kabanov, S. Brazovskii, P. Kusar, J.-H. Chu, I. R. Fisher, and D. Mihailovic, Coherent dynamics of macroscopic electronic order through a symmetry breaking transition, *Nat. Phys.* **6**, 681 (2010).
  - [12] M. Collura and F. H. L. Essler, How order melts after quantum quenches, *Phys. Rev. B* **101**, 041110 (2020).
  - [13] Y. Lemonik and A. Mitra, Quench dynamics of superconducting fluctuations and optical conductivity in a disordered system, *Phys. Rev. B* **98**, 214514 (2018).
  - [14] Z. Sun and A. J. Millis, Pump-induced motion of an interface between competing orders, *Phys. Rev. B* **101**, 224305 (2020).
  - [15] P. E. Dolgirev, A. V. Rozhkov, A. Zong, A. Kogar, N. Gedik, and B. V. Fine, Amplitude dynamics of the charge density wave in  $\text{LaTe}_3$ : Theoretical description of pump-probe experiments, *Phys. Rev. B* **101**, 054203 (2020).
  - [16] P. E. Dolgirev, M. H. Michael, A. Zong, N. Gedik, and E. Demler, Self-similar dynamics of order parameter fluctuations in pump-probe experiments, *Phys. Rev. B* **101**, 174306 (2020).
  - [17] J. Ni and B. Gu, Transient ordered states during relaxation from a quenched disordered state to an equilibrium disordered state, *Phys. Rev. Lett.* **79**, 3922 (1997).
  - [18] J. Ni and B. Gu, The metastable phase diagram and the kinetics of transient ordered states in a ternary system, *J. Phys.: Condens. Matter* **10**, 3523 (1998).
  - [19] H. Gilhøj, C. Jeppesen, and O. G. Mouritsen, Overshooting effects in nonequilibrium ordering dynamics, *Phys. Rev. Lett.* **75**, 3305 (1995).
  - [20] X. Zhang and M. H. F. Sluiter, Kinetically driven ordering in phase separating alloys, *Phys. Rev. Materials* **3**, 095601 (2019).
  - [21] Z. Sun and A. J. Millis, Transient trapping into metastable states in systems with competing orders, *Phys. Rev. X* **10**, 021028 (2020).
  - [22] R. S. MacKay and S. Aubry, Proof of existence of breathers for time-reversible or Hamiltonian networks of weakly coupled oscillators, *Nonlinearity* **7**, 1623 (1994).
  - [23] S. Flach and C. Willis, Discrete breathers, *Phys. Rep.* **295**, 181 (1998).
  - [24] D. K. Campbell, S. Flach, Y. S. Kivshar, *et al.*, Localizing energy through nonlinearity and discreteness, *Phys. Today* **57**, 43 (2004).
  - [25] B. Rumpf, Simple statistical explanation for the localization of energy in nonlinear lattices with two conserved quantities, *Phys. Rev. E* **69**, 016618 (2004).
  - [26] M. Ivanchenko, O. Kanakov, V. Shalfeev, and S. Flach, Discrete breathers in transient processes and thermal equilibrium, *Physica D* **198**, 120 (2004).
  - [27] S. Flach and A. V. Gorbach, Discrete breathers – advances in theory and applications, *Phys. Rep.* **467**, 1 (2008).
  - [28] B. Rumpf, Transition behavior of the discrete nonlinear Schrödinger equation, *Phys. Rev. E* **77**, 036606 (2008).
  - [29] B. Rumpf, Stable and metastable states and the formation and destruction of breathers in the discrete nonlinear Schrödinger equation, *Physica D* **238**, 2067 (2009).
  - [30] Y. Kati, *Equilibrium and Non-equilibrium Gross-Pitaevskii Lattice Dynamics: Interactions, Disorder, and Thermalization*, Ph.D. thesis, Center for Theoretical Physics of Complex Systems, Institute for Basic Science (2021).
  - [31] A. E. Tarkhov, S. Wimberger, and B. V. Fine, Extracting Lyapunov exponents from the echo dynamics of Bose-Einstein condensates on a lattice, *Phys. Rev. A* **96**, 023624 (2017).
  - [32] A. E. Tarkhov and B. V. Fine, Estimating ergodization time of a chaotic many-particle system from a time reversal of equilibrium noise, *New J. Phys.* **20**, 123021 (2018).
  - [33] T. Mithun, Y. Kati, C. Danieli, and S. Flach, Weakly nonergodic dynamics in the Gross-Pitaevskii lattice, *Phys. Rev. Lett.* **120**, 184101 (2018).
  - [34] A. Y. Cherny, T. Engl, and S. Flach, Non-Gibbs states on a Bose-Hubbard lattice, *Phys. Rev. A* **99**, 023603 (2019).
  - [35] A. E. Tarkhov, *Ergodization dynamics of the Gross-Pitaevskii equation on a lattice*, Ph.D. thesis, Skolkovo Institute of Science and Technology (2020).
  - [36] H. H. Rugh, Dynamical approach to temperature, *Phys. Rev. Lett.* **78**, 772 (1997).
  - [37] H. H. Rugh, A geometric, dynamical approach to thermodynamics, *J. Phys. A: Math. Gen.* **31**, 7761 (1998).
  - [38] W. K. den Otter and W. J. Briels, The calculation of free-energy differences by constrained molecular-dynamics simulations, *J. Chem. Phys.* **109**, 4139 (1998).
  - [39] W. K. den Otter, Thermodynamic integration of the free energy along a reaction coordinate in Cartesian coordinates, *J. Chem. Phys.* **112**, 7283 (2000).
  - [40] A. S. de Wijn, B. Hess, and B. V. Fine, Chaotic properties of spin lattices near second-order phase transitions, *Phys. Rev. E* **92**, 062929 (2015).
  - [41] The code is published in a GitHub repository at <https://github.com/TarkhovAndrei/DGPE>.